Thermochimica Acta, 56 (1982) 1–13
Elsevier Scientific Publishing Company, Amsterdam—Printed in The Netherlands

REACTION KINETICS AT LINEARLY INCREASED TEMPERATURE. I. COMPARATIVE CHARACTERIZATION OF REACTIONS IN SOLUTION AND SOLID PHASE IN A UNIQUE "MECHANISTIC DIAGRAM"

E. KOCH

Max-Planck-Institut für Strahlenchemie, D-433 Mülheim a.d. Ruhr (F.R.G.)

(Received 29 October 1981)

ABSTRACT

A complex reaction can be characterized kinetically in a special "Mechanistic Diagram". From a time/rate plot recorded at constant heating, the shape index S and the reaction type index M may be calculated. The latter represents a sort of standardized, reciprocal half-width since it has to be referred to the activation parameters of a reference reaction. In practice, it is useful to take those apparent activation parameters which result from a first-order (or second-order) evaluation of either the initial or the total part of the signal.

In a plane S versus M, all basic sorts of reaction may be recognized since they yield points (first- or second-order elementary processes), lines (e.g. order kinetics, $0 < n < \infty$) or regions. Whereas the regions of homogeneous mechanisms involve at least one of the two elementary points and are often extended, i.e. less specific, the usual heterogeneous models give sharper, isolated regions, often near to the n-order line.

The diagnostic potential of this diagram is strongly increased if parametric curves due to experimental series, based on systematic changes of conditions (initial concentration of reactant, heating rate, pressure etc.) are considered. Constancy of S and M then will signal a temporary dominance of a part of the prevailing reaction mechanism.

INTRODUCTION

Methods of thermal analysis offer a special capability to meet with the problem of "inverse reaction kinetics", i.e. to find out which reaction mechanism is responsible for a kinetic plot observed for a reacting system [1–4]. The reason is that the general involvement of temperature change makes the activation parameters accessible by one experiment.

Activation parameters are nonsensical if the reaction mechanism is not known. A possible way to reveal the mechanism is the generation of theoretical rate curves by the numerical integration of that set of differential equations assumed for the most probable mechanism followed by optimization of the activation and indication parameters (reaction enthalpies, total weight changes or extinction changes [5] etc.) of the particular steps [6–12].

0040-6031/82/0000–0000/$02.75

In practice, such a procedure may need excess computer time since it has to be repeated often for other, perhaps better mechanisms; therefore, this way could be too tedious.

The strategy discussed in this paper is based on the utilization of data gained by a very simple, but preliminary, evaluation of rate curves. It may be applied to TG, DTG, power-compensating DSC and other methods revealing a proportionality between signal and rate of reaction. For DTA curves, performed in an appropriate apparatus, either a transformation to rate curves (using an infinite cell constant) or a correction of data obtained is possible [13–17]. There are two parameters available from experiments which are predominantly dependent on the order or the type of reaction.

(a) The shape index S, i.e. the negative ratio of the slopes of both inflecting tangents. [18–20,57]

(b) The reaction type index M defined in 1973 by the author [21,22] which is based on the approximate proportionality of specific time (u_m) [10,13,14,23] and half-width of an elementary rate curve.

Whilst S is directly available or, in the case of strongly fluctuating curves, may be approximately replaced by the ratio of the tangents at both half-width points [24], the M-index is referred to the activation data of a reference reaction.

$$M = \frac{E}{h(\log k_\infty + \log u_m)^2} \tag{1}$$

where E = activation energy, h = half-width and k_∞ = pre-exponential factor. u_m is calculated using the activation data by iteration

$$u_m = \frac{E}{\Phi R(\ln k_\infty + \ln u_m)^2} \tag{2}$$

where Φ = heating rate and R = gas constant.

For a reaction following a rate law of order n, computer application and experiments involving $n = 1$ and $n = 2$ have confirmed that, for unit initial concentration of reactants [13,14]

$$S = \frac{n^2(1.21 + 0.21n)}{n^2 + 159} \left(\simeq 0.63n^2 \text{ for } n < 1 \text{ [18]}\right) \tag{3}$$

and

$$M = \frac{R}{\log^2 e \times \ln(k_2/k_1)} \simeq \frac{R}{\log^2 e \times 2.25 \times n^{0.52}} \tag{4}$$

where k_1, k_2 = rate coefficients at the half-width points.

Three kinds of reference reactions have been tested for the calculation of the M index from eqn. (1)

(1) using the activation data of the initiating process selected for the computer-generated rate curves (M_{theo}) [22];

(2) using the activation data obtained in the initial range (25% of the time passed) of experimental or theoretical curves by a simple first- or second-order evaluation program (M_{init}); and

(3) as (2) but fitting of the activation data in the total time interval (M_{ov}).

Applied to complex reactions, strategies (2) and (3) lead to apparent activation parameters [1,4,25,26]. Despite this, the M values are useful since they, analogously to the S values, reveal the character of the deviations from the "elementary" M values expressed by eqn. (4) and, hence, are descriptive of the kind of reaction mechanism.

Consequently, a diagram formed by the "mechanistic" coordinates S and M offers an extraordinary capability for a kinetic discussion of reactions. This was confirmed by results from a series of experiments using various systems in solution involving different initial concentrations of reactant. The values of 13 parameters of kinetic relevance plotted vs. initial concentration have shown that the S and M values possess the maximum number of periods of constancy (cf. refs. 1 and 4). Such periods, however, must directly reflect the rate-determining steps of the reaction mechanism in the prevailing range of concentration. On the contrary, parameters such as temperature or overall enthalpy are very inefficient. Data such as the initial or the overall activation energy or the corresponding pre-exponential factors show a medium number of such periods, but often do not represent true alternatives to each other.

COMPUTER APPLICATION

In theoretical and experimental approaches to non-isothermal reaction kinetics, computer programs were developed for the evaluation of signals, numerical integration for adapting theoretical to experimental curves, specified search of experimental files and graphic representation of the correlations of any selected parameters of so-called experimental series (Fig. 1) [10,14,16,27]. The programs are linked with a computer library in which all experimental and (intermittently) theoretical plots are stored, including 18 input and 41 result parameters each. This high expenditure in data processing facilities favors finding the optimum way for evaluation and interpretation of experiments. The concept avoids high calculation times for generating and adapting model curves for each individual experiment, but instead requires the creation of unique mechanistic maps for a direct comparison of this experiment with theory.

Homogeneous reaction mechanisms

In a first stage, all possible two-reaction models (cf. ref. 21) were studied. The activation data of the initiating process were taken constant ($E_1 = 15$

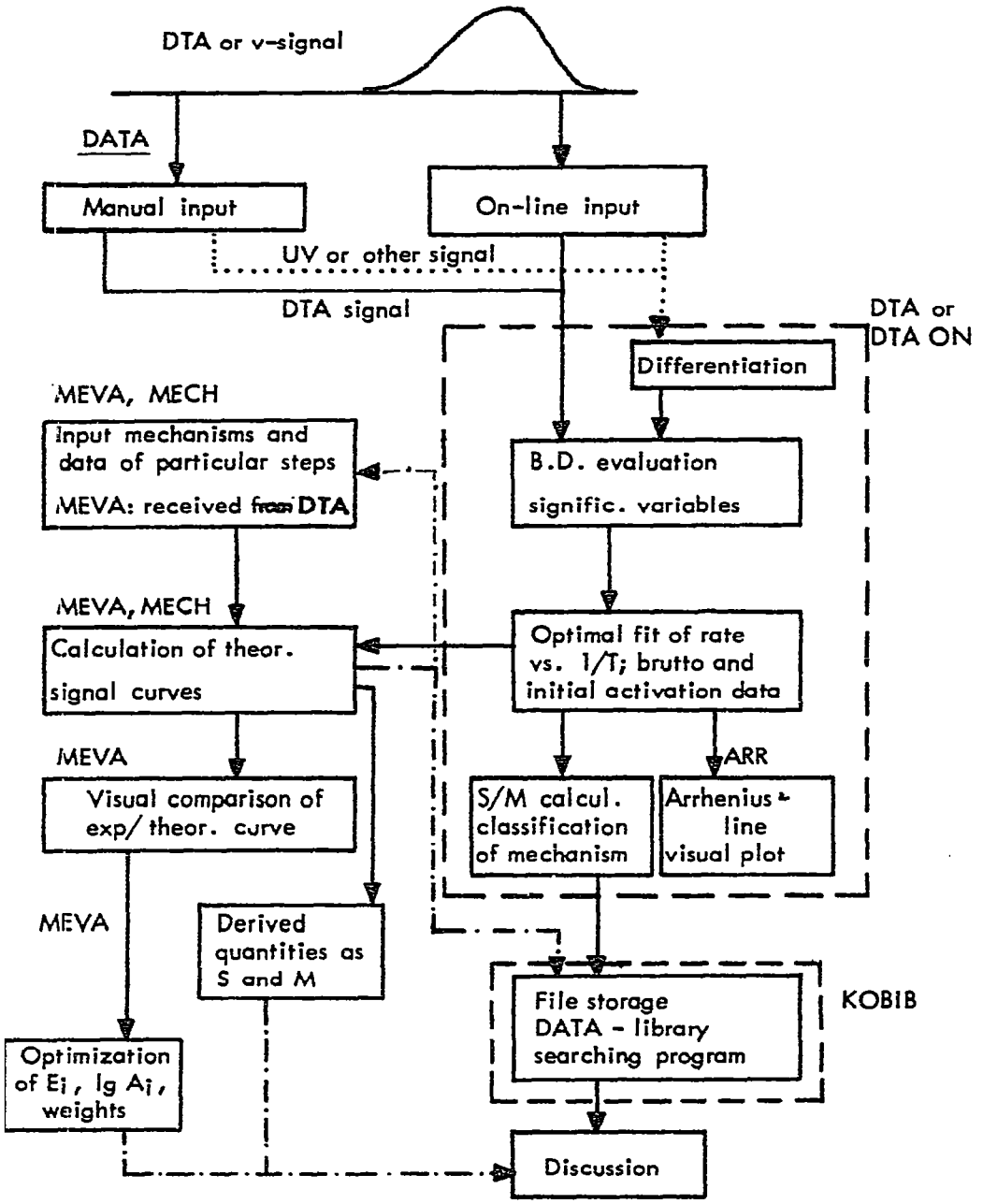

Fig. 1. Block scheme of computer programs.

kcal mole^{-1}, log $k_{\infty 1} = 12$, time = min, $\Phi = 1.5$ K min^{-1}) while log $k_{\infty 2}$ was set to either 4, 8, 12 or 16 for one series which may cover the realistic range of possible values. E_2 was varied in steps, beginning at a low value excluding an observed interference by the other process, and ending at so high a value that the interference had disappeared. Individual evaluation of the model curves using the order of the initiating process ($n = 1$ or 2) yielded the shape index and both the initial- and overall-referred M index. Plotting of the resulting S/M-points for a unique pre-exponential factor leads to a line in

the S/M diagram with E_2 as the prevailing parameter. The totality of the four parametric lines indicates a realistic region characteristic of the model considered.

A mechanistic map produced in this way is generally applicable, because, if the data of a real initiating reaction differ from the standard values, a simple recalculation of the data of the second reaction must leave the position of the mechanistic point nearly unchanged [24]. If the heating rate Φ' differs from the standard value, then the activation data of both processes may be corrected using the formulae

$$E' = E\frac{1.5}{\Phi'} \tag{5a}$$

$$\log k'_\infty = \log k_\infty + \log\frac{\Phi'}{1.5} \tag{5b}$$

in order to use the standard diagram when a second correction to the standard initiating reaction from above has been performed.

Heterogeneous reaction mechanisms

Validity of the general equation [4,11,28–31]

$$\frac{d\alpha}{dt} = k(T)(1-\alpha)^n\alpha^m\left[-\ln(1-\alpha)\right]^p \tag{6}$$

was assumed which includes the most important mechanisms discussed in the literature (Table 1).

TABLE 1

Basic rate laws of solid-phase reactions

Code	Exponents in eqn. (6)			Mechanism
	m	n	p	
Phase-boundary controlled reactions				
R1	0	0	0	One-dimensional movement (Polanyi–Wigner)
R2	0	1/2	0	Two-dimensional movement
R3	0	2/3	0	Three-dimensional movement
Diffusion-controlled reactions				
D1	−1	0	0	Parabolic law: One-dimensional diffusion
D2	0	0	−2	Two-dimensional diffusion
D3	0	1/3	−1	Three-dimensional diffusion
Nucleation-controlled reactions				
NP1	≤1	0	0	Nucleation power law: $m = 1/4, 1/3, 1/2, 1$
A2	0	1	1/2	Two-dimensional growth of nuclei (Avrami)
A3	0	1	2/3	Three-dimensional growth of nuclei (Avrami)
NPT	1	1	0	Prout–Tompkins mechanism
NLX	<<−1	0	0	Explosive/branched reactions

Model curves were calculated using activation energies of 10, 15 and 30 kcal mole^{-1}, the logarithmic frequency factors from above (4, 8, 12 and 16) and $\Phi = 1.5$ K min^{-1}, again.

Equation (6) contains only *one* rate coefficient, $k(T)$. In spite of this formal absence of a second process, a reference process was created as that first-order reaction which involves the same activation parameters obtained by an elementary evaluation program of first order. Justification of this procedure may be derived from the fact that for a first-order process the initial concentration of the reactant does not intrude into the resulting pre-exponential factor, which is in agreement with the usual standardization caused by the use of the fractional conversion, α. Furthermore, at the onset of an experimental rate curve the order has no influence on the activation energy calculated so that M values referred to in this way may represent a realistic measure of the later deviations from an "elementary" advancement of the process.

RESULTS OF THE SIMULATIONS

In Fig. 2, S/M regions of the possible two-reaction mechanisms, starting from one reactant, are shown. For each mechanism, three "model maps" based on a horizontal linear scale for S and a vertical linear scale for M are plotted due to the three reference modes discussed (selection of M_{theo}, M_{init} or M_{ov}). The elementary points for both a first- and second-order process have been repeated in all pictures to facilitate the orientation.

Apart from the two-reaction mechanisms, some special "quasielementary" reactions are also shown, namely the normal bimolecular process A + B → products (= AB; $[A]_0 \neq [B]_0$; a region joining one elementary point with the other), the autocatalytic bimolecular process A + B → 2 B(= 1a; approximately a line according to the concentration ratio $[A]_0$:$[B]_0$) and the "n-order" process n A → products (a line of positive curvature passing through both elementary points, see Fig. 3).

The borders of the regions are not strict; they may give the limits for reasonable activation data. Dash lines signal either a splitting of one peak into two on increased E_2 value, or the start of a complementary region, e.g. P_{21} instead of P_{12} when the second-order process begins to dominate at the onset of the process (initial temperature). In the case of opposing reactions (= G), the dark fields involve exothermic reactions ($E_2 > E_1$), whereas dash limiting lines corresponding to the white (endothermic) fields indicate that the signal height will tend to zero on surpassing the lines because of the compensation of the opposite signal effects (21,22,32].

All *homogeneous* mechanisms correspond to regions involving either one or both elementary points. The distance of a mechanistic point from an elementary point is a measure of the kinetic interference of the "nearest"

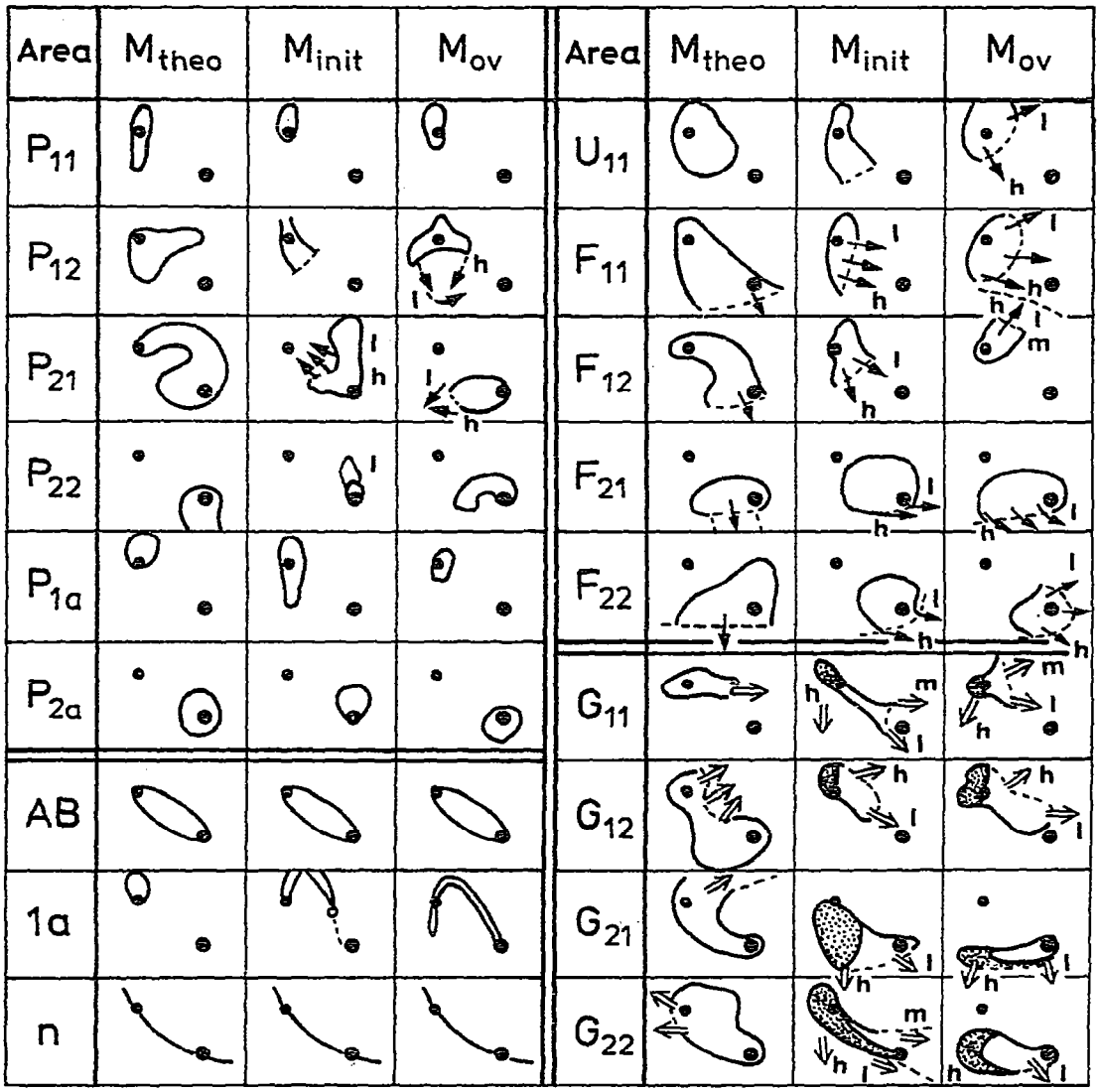

Fig. 2. Mechanistic regions of homogeneous two-reaction models. P, competitive; U, independent; F, consecutive; G, opposing reactions. Indices: reaction orders of the partial steps in the order of occurrence, starting from low temperature. AB, process A+B→products; 1a, process A+B→2B; *n*, process of order *n*, *n*A→products. →separation, ⇒disappearance of signals

particular process by the other(s). Consequently, for mixed-order processes based on fixed activation data, *limiting cases* must exist since, for very low or very high initial concentration of reactant, the elementary points ① and ② are reached [22,33]. Analogously, in certain mechanisms other parametric lines may appear for a variation in the heating rate [33–36].

For the comparative representation of the *heterogeneous* mechanisms, a special arctan scale was used for the *M* value [Figs. 3(a) and (b)]. The initial-referred heterogeneous regions [Fig. 3(a)] are often sharper than the homogeneous ones and reveal no linkage to the elementary points. They are

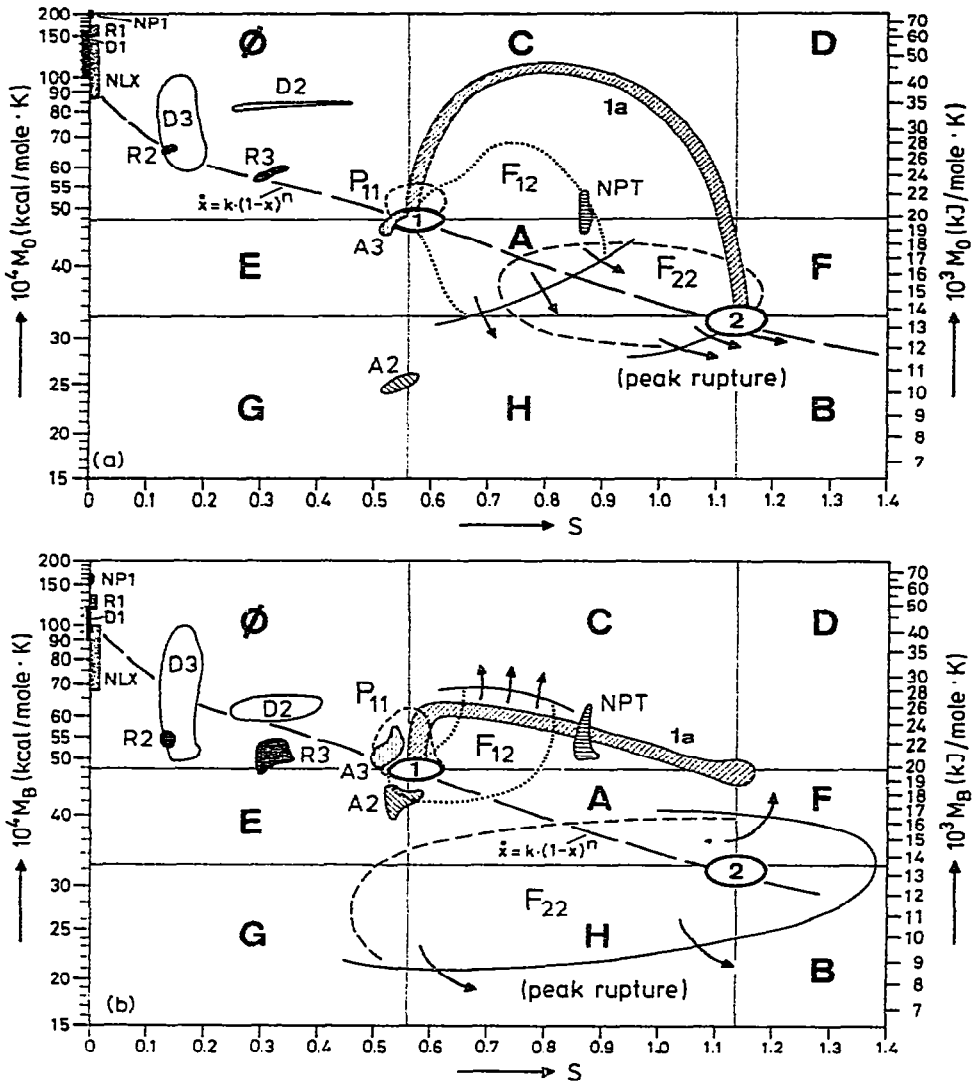

Fig. 3. Mechanistic (a) initial and (b) overall diagram. Abbreviations: *see* Table 1. M scale: $y \sim \arctan [1+(M-0.005)\times 300]+3$. Some homogeneous mechanisms have been included (cf. Fig. 2).

often located near the "n-order line", which agrees with the general experience that many solid-phase reactions can approximately be described by mass action kinetics [37–39]. Furthermore, the majority of the heterogeneous mechanisms is located in the field ϕ of Fig. 3 ($n < 1$) or may even show a sort of "zero-order" behaviour (models R1, NLX, NP1, D1).

In arbitrary cases hitherto studied, an increase in the heating rate from 1.5 to 5 has no dramatic effect on the position of the initial-referred regions. In contrast, the overall-referred regions [Fig. 3(b)] are often strongly displaced by a change in the heating rate. In spite of this, the additional use of these regions is to be recommended for the discrimination of similarly placed mechanisms, such as A3 and ①, D2 and R2 or D1 and NLX [40–42].

Quantitative application of the mechanistic maps from above requires experiments in an ideal apparatus characterized by homogeneity in temperature, exact validity of the selected temperature program and absence of intruding properties of sample or apparatus. In solid-phase studies, such conditions are hard to realize [26,43], but a study of mechanistic curves produced by variation of a parameter of apparatus or sample may contribute to estimating the "absolute" converging points from the relative S/M indices.

DISCUSSION

Values of the mechanistic coordinates of various reactions have been given recently [14,22,44–49]. However, a utilization of the true potential of mechanistic master diagrams must include experimental series for different initial concentrations and/or heating rates [36]. In Table 2, some examples of the results of such concentration series are presented. Rectangular (or oval, as ① and ②) fields as defined in Figs. 3(a) and (b) are listed in the order of their first contact with the mechanistic curves generated in particular experiments at increasing initial concentration of one reactant. Although correlation coefficients of > 0.99 were observed for the Arrhenius straight-line fit in some cases (which implies a formal similarity of the curves), the mechanistic codes are totally different, but may be compared with those of simulated experiments.

In further contributions of this series, various experimental examples of complex reactions in solution will be discussed in detail.

An example of application in the solid phase is the thermal decomposition of nickel oxalate [40]. For a theoretical signal curve based on the published data ($E = 100.5$ kJ mole^{-1}, $k_\infty = 1.4 \times 10^{10}$ s^{-1}, estimated for $\Phi = 5$ K min^{-1} and $\alpha_0 = 0.12$), a first-order re-evaluation leads to the mechanistic coordinates $M_{\text{init}} = 0.0185$ kJ mole^{-1} K^{-1} and $S = 0.869$, corresponding to a point somewhat below the Prout–Tompkins region, NPT. However, if a model curve based on the standard heating rate, $\Phi = 1.5$ K min,$^{-1}$, is used, one obtains $M_{\text{init}} = 0.0201$, which, indeed, contacts the NPT region in Fig. 3(a), because S remains unchanged.

In contrast, the overall M index reveals a dramatic increase with the heating rate ($M_{\text{ov}} = 0.0469$ for $\Phi = 5$). The experiments were performed using Φ values between 5 and 20 K min^{-1}; therefore, Fig. 3(b) seems not to be generally applicable and the influence of Φ has to be studied in more detail in order to test whether a unique diagram applicable in the broad range of usual heating rates can be developed.

General application of the method presented surely requires additional computer work at a larger scale. Such an extension seems attractive because the mathematical source responsible for the success of the procedure is the

TABLE 2

Mechanistic concentration codes for some reactions in solution

The mechanistic fields (Abbreviations: Fig. 3) are listed for the lowest concentration at the entry of the parametric curve. Region Ⓘ: $M = \bar{M}_2 = 0.013$; $S = S_1 = 0.58$; region Ⓘ: $M = \bar{M}_1 = 0.019$; $S = S_2 = 1.15$.

Double symbols (e.g. $\overline{AC}$) denote separating horizontal or vertical straight lines in the diagram. O, loop; ——— or ●, intermediate stop or convergence point; — — —, M is constant; ·····, S is constant; Ph, phenyl.

Variable reactant	Molarity of constant reactant(s)	Solvent	M Order	Concentration of variable reactant→						
				10^{-5}	10^{-4}	10^{-3}	10^{-2}	10^{-1}	10^{0}	10^{1}
Cyclohexadiene-(1,3)	0.055 $(OPh)_3PO_3$	CH_2Cl_2	M_{20}				Ⓘ	A $\overline{AC}$ E	Ⓘ	G→
			M_2				E	A C	E Ⓘ	$\overline{ØE}$–●
$(OPh)_3P$	0.055 $(OPh)_3PO_3$	CH_2Cl_2	M_{20}				$\overline{ØC}$ Ø E G H B H →			
			M_2				$\overline{ØC}$ Ø E G H 2 F A →			
O_3		$(i\text{-}C_3H_7)_2O$	M_{10}				D C ⒾC ●			
			M_1				D C ⒾC $\overline{AC}$ ●			
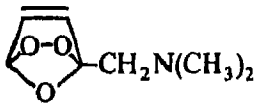		CH_3OH	M_{10}			AC Ø EⒾA ⒾØ E C ●				
			M_1			A $\overline{AC}$ C Ø $\overline{ØE}$ E A $\overline{AC}$ Ø —●				
$KMnO_4$	0.075 $CH_2(COOH)_2$	aq.H_2SO_4	M_{20}			Ø E A C A ● A				
			M_2			Ø E A -O- A →				
$NaBrO_3$	0.0345 NaBr	aq.H_2SO_4	M_{20}			C Ø Ⓘ C D Ⓘ $\overline{AC}$ A ●				
	0.375 $CH_2(COOH)_2$		M_2			C I E A F C				
	0.025 $Ce(SO_4)_2$									
$MnSO_4$	0.0675 $NaBrO_3$	aq.H_2SO_4	M_{20}	Ø -●- Ø -●- C D $\overline{FD}$ Ⓘ D →						
	0.375 $CH_2(COOH)_2$		M_2	Ø -O-Ⓘ $\overline{AC}$ D $\overline{FD}$ D C D →						
	0.0375 NaBr									

same as in the concept of master curves, based on a reduced reaction time [29,43,50–52]. This quantity was referred to a certain fraction of the total conversion, namely half of it. The M index is determined by both half-width temperatures, which for an elementary process always corresponds to fixed fractional conversions, e.g. $\alpha_1 = 0.39$ and $\alpha_2 = 0.90$ for a first-order reaction [10,23]. The desirable universal role of the half-width as an exclusive function of the reaction order is reached by defining the M index as referred to the activation parameters of the reaction, eqn. (1). On the other hand, profit is also taken from the suggestions of Selvaratnam and Garn to consider the rate of conversion against such a reduced time, instead of the conversion itself [34,53].

In contrast to the method of master curves, the author's method of comparing an S/M point (as a geometric equivalent of the type of reaction studied) with a model map of reaction mechanisms, has the disadvantage that, obviously, only five fractions of the experimental rate curve are really utilized, those at the maximum, at both half-width points and both points of inflection. However, additional information used for the calculation of M stems from the initial and/or total range of the curve. In addition, if a series of experiments were performed with a systematic change of conditions [11,43], this will lead to a parametric curve which may show limiting points and/or intermediate stops indicating fractional units of the whole reaction mechanism [1,4,10,54]. In *homogeneous* kinetics, taking the initial concentration as the condition parameter offers excellent chances for a successful application of the mechanistic diagram. In *heterogeneous* kinetics, such a procedure is more difficult to realize, e.g. by mixing the sample with a pulverized diluent or by performing a previous partial conversion, whereas variation of the heating rate or other parameters (as pressure, sample size [55] etc) in accordance with computer simulations will represent a powerful tool for the kinetic characterization of a reaction [2,10,22,34,43,56–57].

ACKNOWLEDGEMENT

I am grateful to Mrs. G. Mummerz for her assistance in the generation of model curves by the use of a PDP 10 computer of the Digital Equipment Corp., Maynard, MA, U.S.A.

REFERENCES

1 E. Koch, The Problem of Inverse Reaction Kinetics under the Aspect of Calorimetric Measurements. Presented on Ulmer Kalorimetrietage, April 6–7th, 1981, Ulm, West Germany; Thermochim. Acta, 49 (1981) 25.
2 E. Koch, Non-isothermal Reaction Analysis, Academic Press, London, 1977

3 E. Koch, in K.H. Ebert, P. Deuflhard and W. Jäger (Eds.), Modelling of Chemical Reaction Systems, Springer Series of Chemical Physics, Vol. 18, Springer, Berlin, 1981, pp. 216–225.
4 E. Koch, Angew. Chem., in press.
5 E. Koch and B. Stilkerieg, in E. Marti, H.R. Oswald und H.G. Wiedemann (Eds.), Angewandte Chemische Thermodynamik und Thermoananalytik, Birkhäuser, Basel, 1979, pp. 210–215.
6 D.D. Warner, J. Phys. Chem., 81 (1977) 2329.
7 D. Edelson, J. Chem. Educ., 52 (1975) 642.
8 R.M. Noyes, J. Phys. Chem., 81 (1977) 2315.
9 M.B. Carver and A.W. Boyd, Int. J. Chem. Kinet., 11 (1979) 1097.
10 E. Koch, in E. Marti, H.R. Oswald und H.G. Wiedemann (Eds.), Angewandte Chemische Thermodynamik und Thermoanalytik, Birkhäuser, Basel, 1979, pp. 141–147.
11 P.D. Garn, Thermochim. Acta, 5 (1973) 485.
12 J. Plewa, J. Norwicz, N. Hajduk and M. Romanska, Thermochim. Acta, 46 (1981) 217.
13 E. Koch and B. Stilkerieg, Thermochim. Acta, 17 (1976) 1.
14 E. Koch and B. Stilkerieg, Thermochim. Acta, 27 (1978) 69.
15 E. Koch, B. Stilkerieg and L. Carlsen, Thermochim. Acta, 33 (1979) 387.
16 E. Koch, B. Stilkerieg and L. Carlsen, Ber. Bunsenges. Phys. Chem., 83 (1979) 1238.
17 R.C. Reed, L. Weber and B.S. Gottfried, Ind. Eng. Chem. Fundam., 4 (1965) 38.
18 H.E. Kissinger, Anal. Chem., 29 (1957) 1702.
19 H. Anderson, D. Haberland and E. Witte, Z. Chem., 18 (1978) 153.
20 J.M. Criado, P. Malet, G. Munvera and V. Rives-Arnau, Thermochim. Acta, 38 (1980) 37.
21 E. Koch, Chem. Ing. Tech., 44 (1972) 111.
22 E. Koch Angew. Chem., 85 (1973) 381; Angew. Chem. Int. Ed. Engl., 12 (1973) 381.
23 E. Koch, Non-isothermal Reaction Analysis, Academic Press, London, 1977, pp. 90–117.
24 E. Koch, unpublished results.
25 P.D. Garn, J. Therm. Anal., 10 (1976) 99.
26 P.D. Garn, Thermochim. Acta, 28 (1979) 185.
27 E. Koch and B. Stilkerieg, J. Therm. Anal., 17 (1979) 395.
28 J. Šesták and G. Berggren, Thermochim. Acta, 3 (1971) 1.
29 J.H. Sharp, G.W. Brindley and N.A. Achar, J. Am. Ceram. Soc., 47 (1966) 379.
30 J. Šesták, V. Satava and W.W. Wendlandt, Thermochim. Acta, 7 (1973) 1.
31 D. Dollimore, G.R. Heal and B.W. Kruplay, Thermochim. Acta, 24 (1978) 293.
32 E. Koch, Non-isothermal Reaction Analysis, Academic Press, London, 1977, pp. 146–152, 195–196.
33 E. Koch, Non-isothermal Reaction Analysis, Academic Press, London, 1977, pp. 160–165, 290–292.
34 J.H. Flynn and L.A. Wall, J. Res. Natl. Bur. Stand. Sect. A, 70 (1966) 487.
35 J.H. Flynn, Thermochim. Acta, 37 (1980) 225.
36 E. Koch, Non-isothermal Reaction Analysis, Academic Press, London, 1977, pp. 386–387.
37 J.H. Sharp, in R.C. Mackenzie, (Ed.), Differential Thermal Analysis Vol. 2, Academic Press, London, 1977, pp. 61–62.
38 A.C. Norris, M.I. Pope and M. Selwood, Thermochim. Acta, 41 (1980) 357.
39 E. Koch, Non-isothermal Reaction Analysis, Academic Press, London, 1977, p. 22.
40 J.M. Criado, F. Gonzalez and J. Morales, Thermochim. Acta, 12 (1975) 337.
41 J.M. Criado and J. Morales, Thermochim. Acta, 19 (1977) 305.
42 J.M. Criado and J. Morales, Thermochim. Acta, 41 (1980) 125.
43 P.D. Garn, J. Therm. Anal., 13 (1978) 581.
44 E. Koch, Anal. Chem., 45 (1973) 2120.
45 E. Koch, J. Therm. Anal., 6 (1974) 483.
46 L. Carlsen, A. Holm, E. Koch and B. Stilkerieg, Acta Chem. Scand. Ser. B, 31 (1977) 679.

47 E. Koch, Non-isothermal Reaction Analysis, Academic Press, London, 1977, pp. 355–379, 541–547.
48 E. Koch and B. Stilkerieg, Thermochim. Acta, 29 (1979) 205.
49 P. Lechtken, Chem. Ber., 109 (1976) 2862.
50 J. Behnisch, E. Schaaf and H. Zimmermann, Thermochim. Acta, 42 (1980) 65.
51 L.F. Jones, D. Dollimore and T. Nicklin, Thermochim. Acta, 13 (1975) 240.
52 J.M. Criado, Thermochim. Acta, 24 (1978) 186.
53 M. Selvaratnam and P.D. Garn, J. Am. Ceram. Soc., 59 (1976) 376.
54 E. Koch and B. Stilkerieg, Proc. 6th Int. Conf. Therm. Anal., Bayreuth, July 6–12, 1980, Birkhäuser, Basel, 1980.
55 P.K. Gallagher and D.W. Johnson, Jr., Thermochim. Acta, 6 (1973) 67.
56 K. Heide, G. Kluge and V. Hlawatsch, Thermochim. Acta, 36 (1980) 151.
57 H. Jüntgen and K.H. van Heek, Fortschr. Chem. Forsch., 13 (1970) 601.